Supplementary Figures and Tables

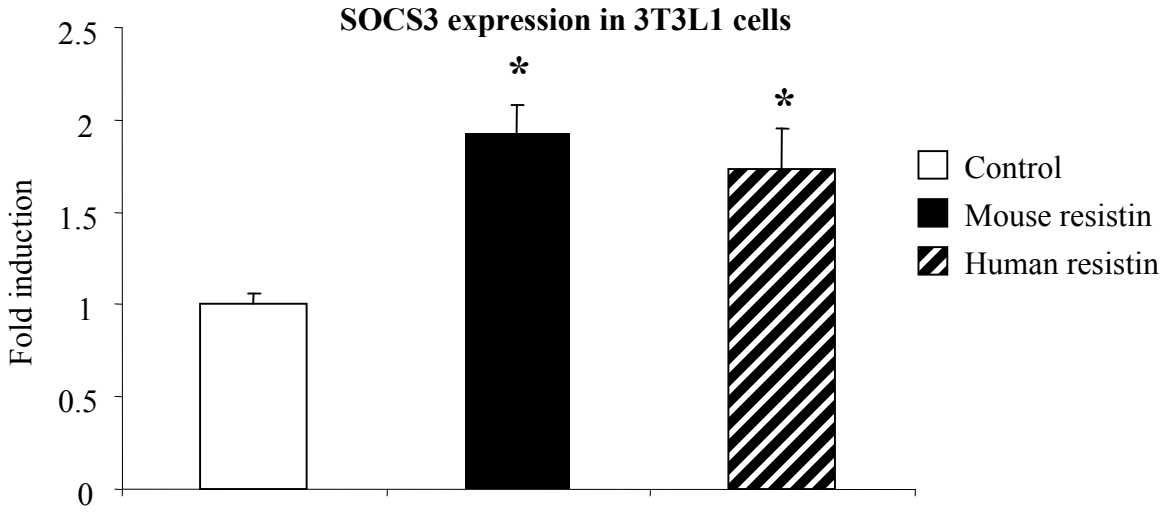

Figure S1. Human resistin activates SOCS-3 expression in mouse 3T3L1 adipocytes. Similar to mouse resistin, human resistin induces SOCS-3 expression in 3T3L1 adipocytes. Real-time RT-PCR was used to measure mRNA levels. Data are expressed as mean ± SEM; n = 5, * $P < 0.05$.

Genotype	Expected	Observed
Control Mice (retn -/-)	100	96
Humanized Resistin Mice (retn -/-; CD68-human resistin)	100	104

Supplementary table. Genetic analysis of pups. Genetic analysis of the first 200 pups resulting from the crosses to generate the humanized resistin mice.

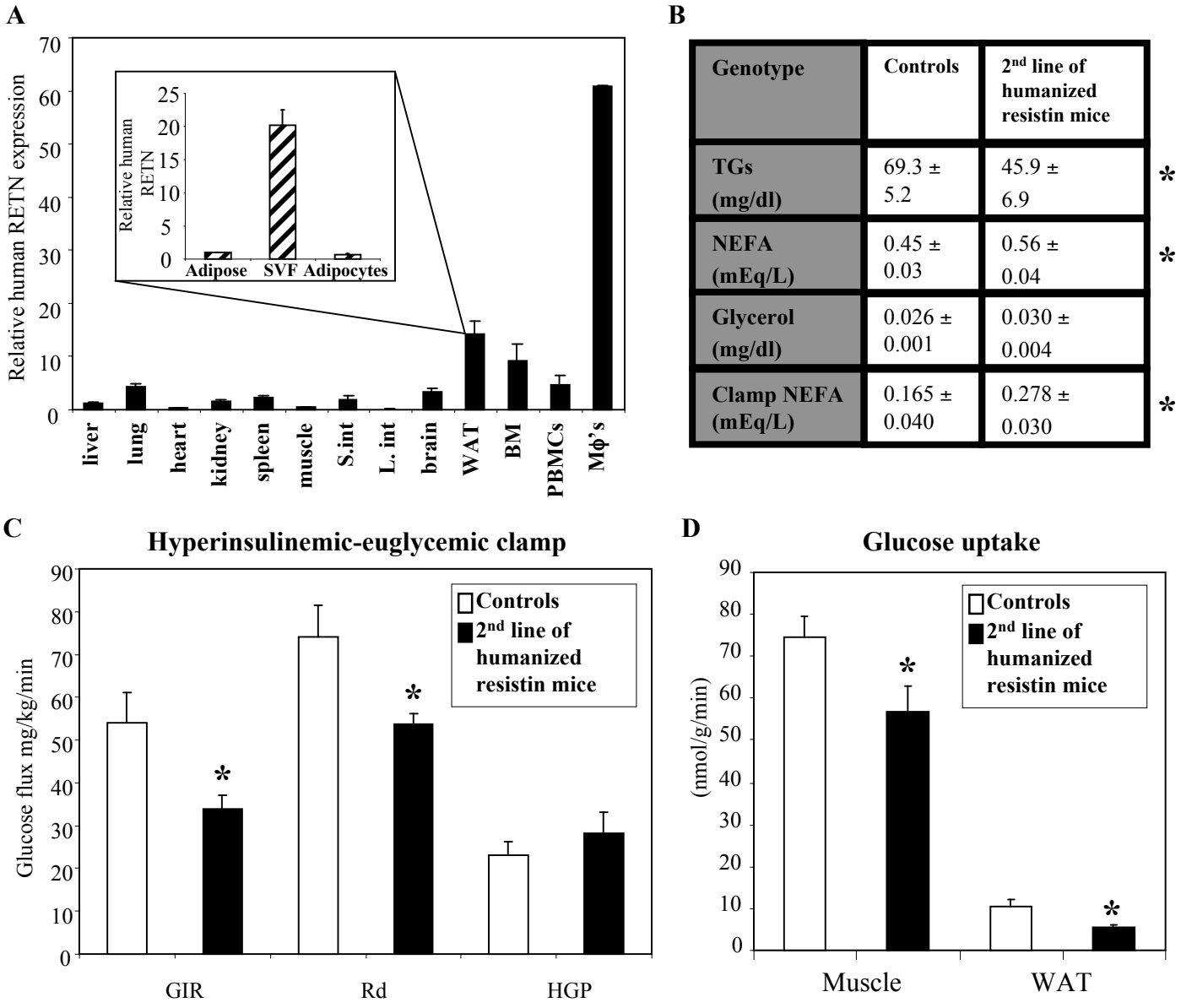

Figure S2. Analysis of the 2nd line of humanized resistin mice. (**A**) The expression pattern of human resistin in the 2nd line resembles that of the 1st line of humanized resistin mice. As expected, human resistin is highly expressed in macrophages (Mϕ's) as well as peripheral blood mononuclear cells (PBMCs) and bone marrow (BM), and the majority of the expression in WAT originates from the SVF ; n = 5. (**B**) Serum chemistry profile of the 2nd line of humanized resistin mice. Similar to the first line, the 2nd line of humanized resistin mice have a serum profile indicative of increased lipolysis with significantly higher serum FFAs levels. Clamp (NEFA) is serum non-esterified fatty acids under hyperinsulinemic-euglycemic clamp conditions, which shows that the 2nd line of humanized resistin mice show resistance to insulin's ability to suppress lipolysis in WAT; n = 6, * $P < 0.05$. (**C**) Hyperinsulinemic-euglycemic clamp analysis of the 2nd line of humanized resistin mice v. retn $^{-/-}$ controls shows decreased GIR and decreased Rd similar to the first line. *$P<0.05$; n =4-6. (**D**) The 2nd line of humanized resistin mice had decreased rate of insulin-stimulated glucose uptake in muscle and WAT compared to retn $^{-/-}$ control littermates. Data are expressed as mean ± SEM; n =4-6. *TGs*: Triglycerides, *GIR*: glucose infusion rate, *Rd*: rate of glucose disposal, *HGP*: hepatic glucose production, *WAT*: white adipose tissue, *SVF*: stromovascular fraction.

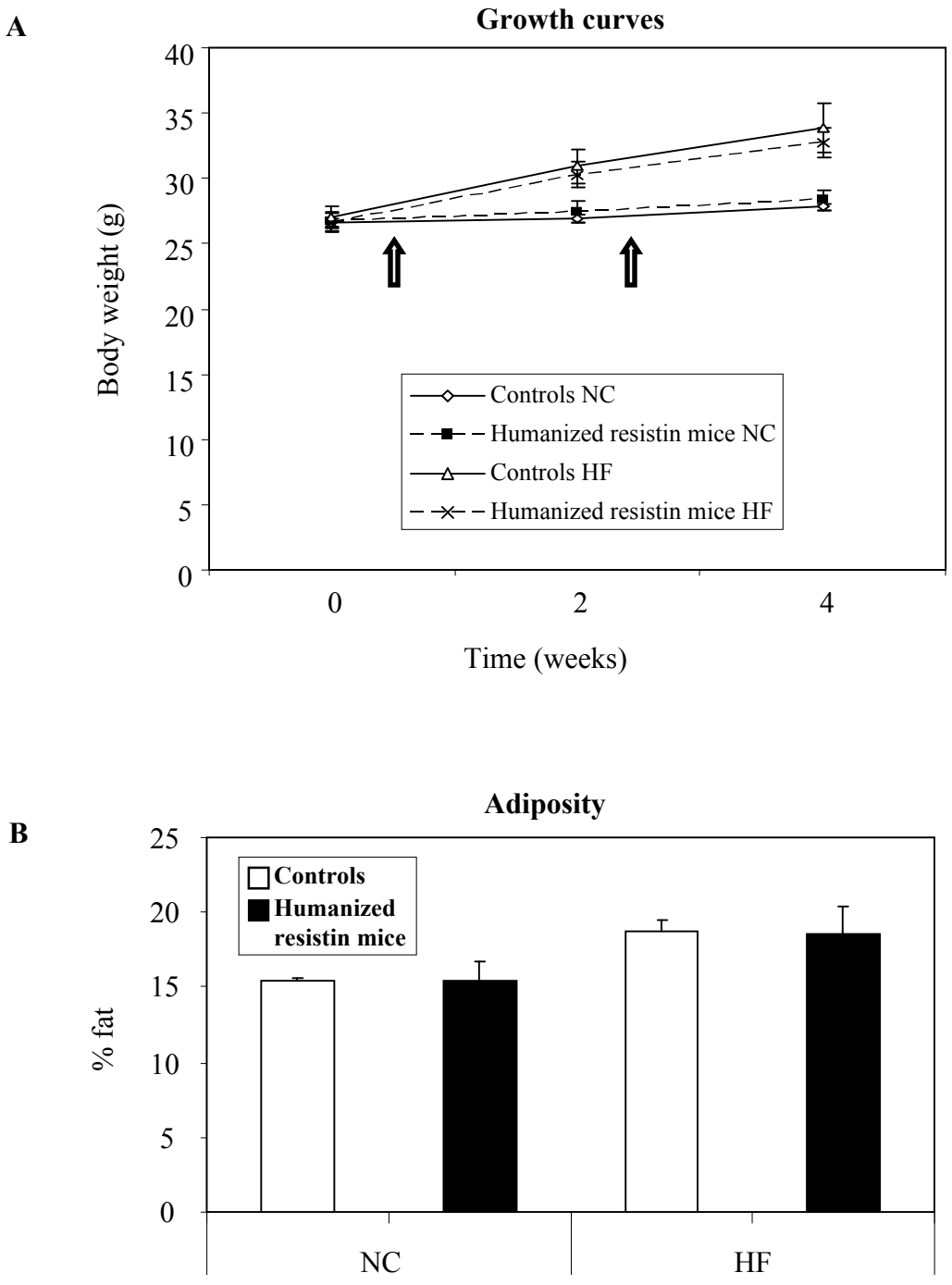

Figure S3. Growth curves of mice on normal chow and high fat diet and adiposity of high fat diet fed mice. (A) Control and humanized resistin mice were put on normal chow or high fat diet. Arrows indicate the time points were the mice were analyzed in our studies. Data are expressed as mean ± SEM; $n = 16$. **(B)** Adiposity of control and humanized resistin mice on high fat diet for 2-3 weeks as measured by NMRI. *NC*: Normal chow diet, *HF*: High fat diet, *NMRI*: Nuclear Magnetic Resonance Imaging. Data are expressed as mean ± SEM; $n = 4$.

A

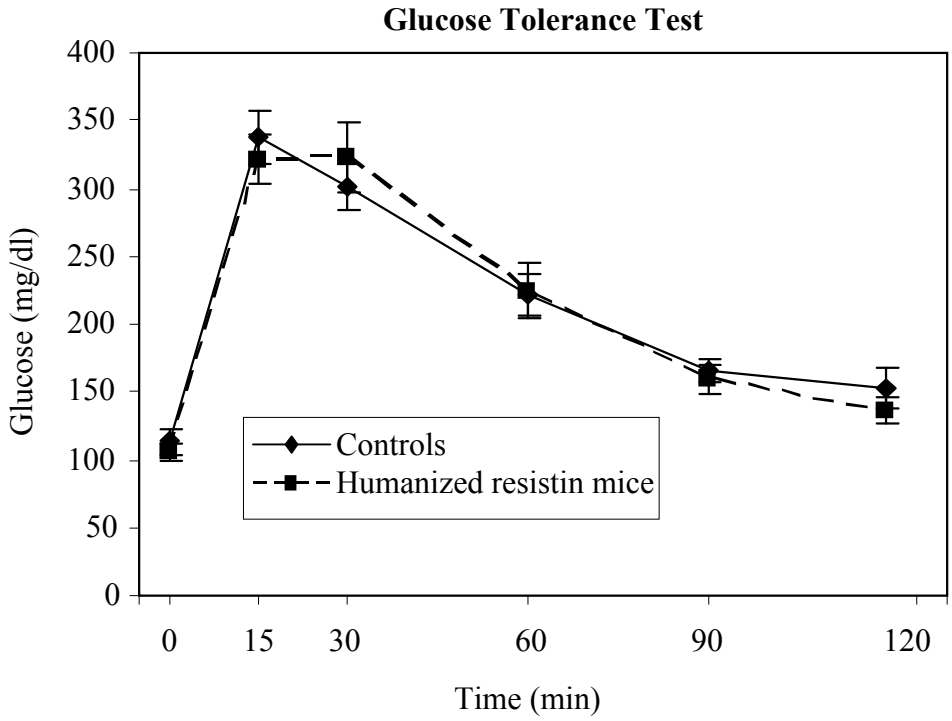

B

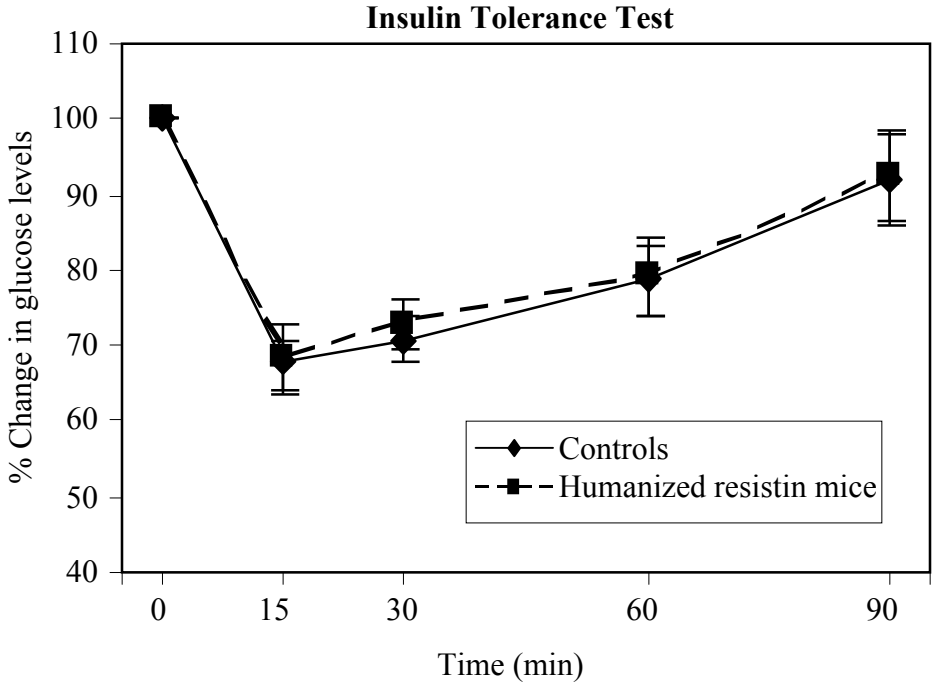

Figure S4. Glucose homeostasis in humanized resistin mice on normal chow. (**A**) Humanized resistin mice show no difference in glucose tolerance or (**B**) insulin tolerance under normal chow fed conditions compared to controls. Data are expressed as mean ± SEM; $n = 8$.

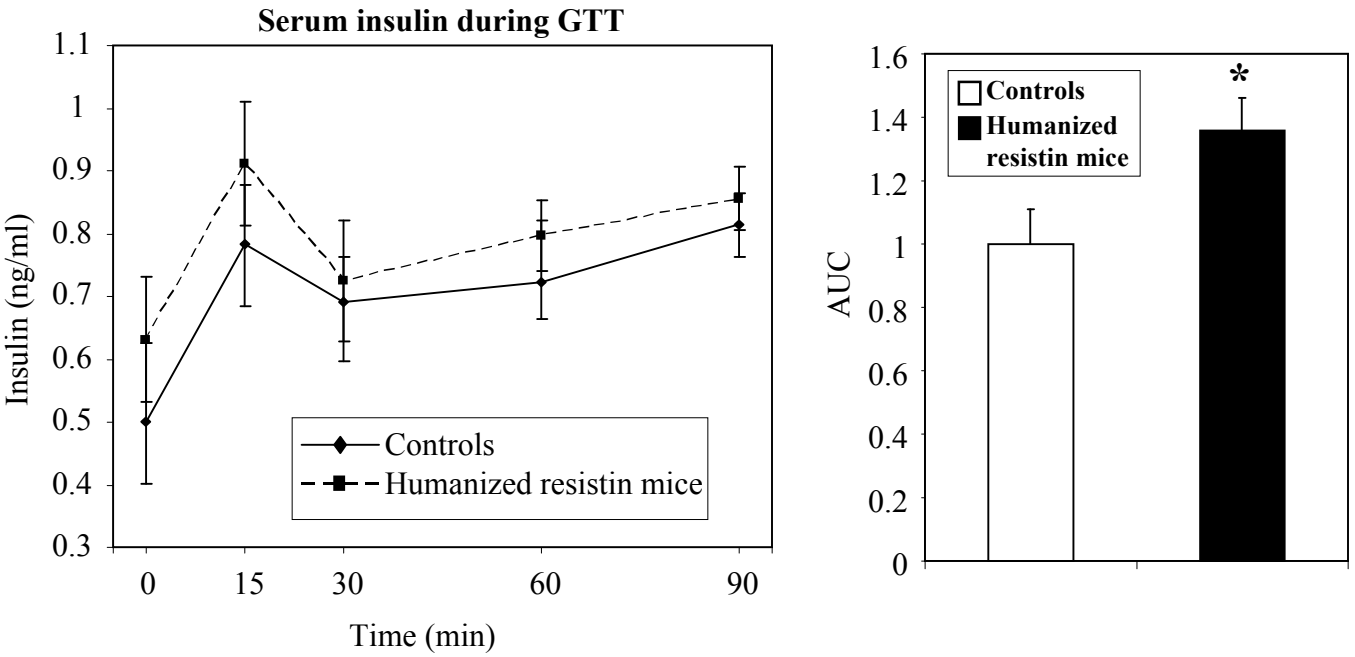

Figure S5. Serum insulin levels during glucose tolerance test. Serum insulin levels during GTT (left) show that the humanized resistin mice tended to have higher insulin levels after a glucose challenge. This difference was statistically significant as measured by area under the curve (right) normalized to control animals. *GTT*: Glucose Tolerance Test, *AUC*: Area Under the Curve. Data are expressed as mean ± SEM; $n = 7$, * $P < 0.05$.

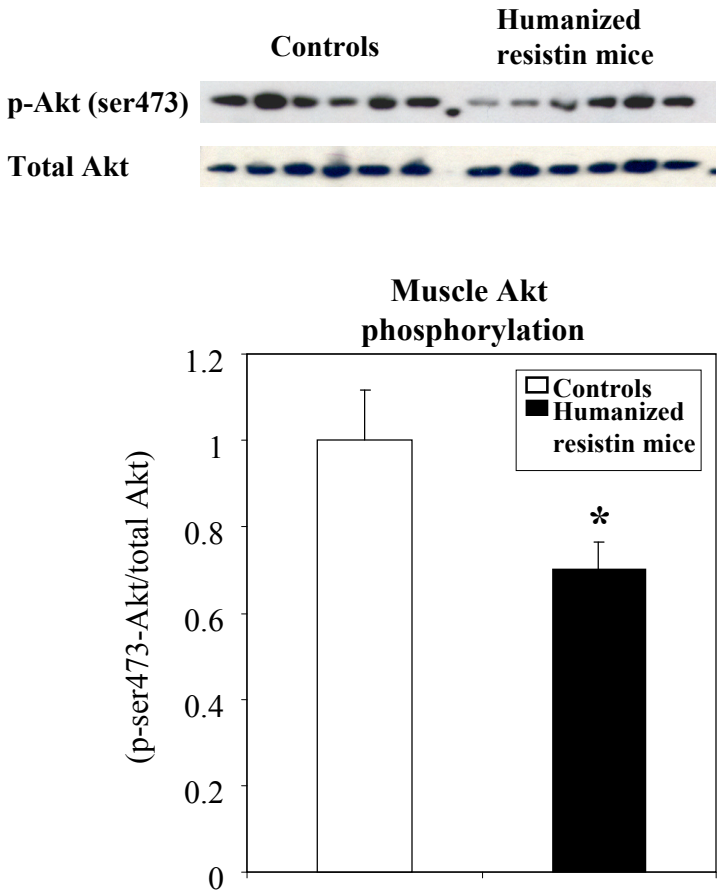

Figure S6. Decreased insulin stimulated Akt ser 473 phosphorylation in muscle. Western blot analysis of muscle of humanized resistin mice compared to control mice under clamped conditions shows a decrease in Akt ser 473 phosphorylation indicative of insulin resistance (top). The blot was quantified (bottom) and normalized to controls. *P<0.05 Data are expressed as mean ± SEM; n = 6.

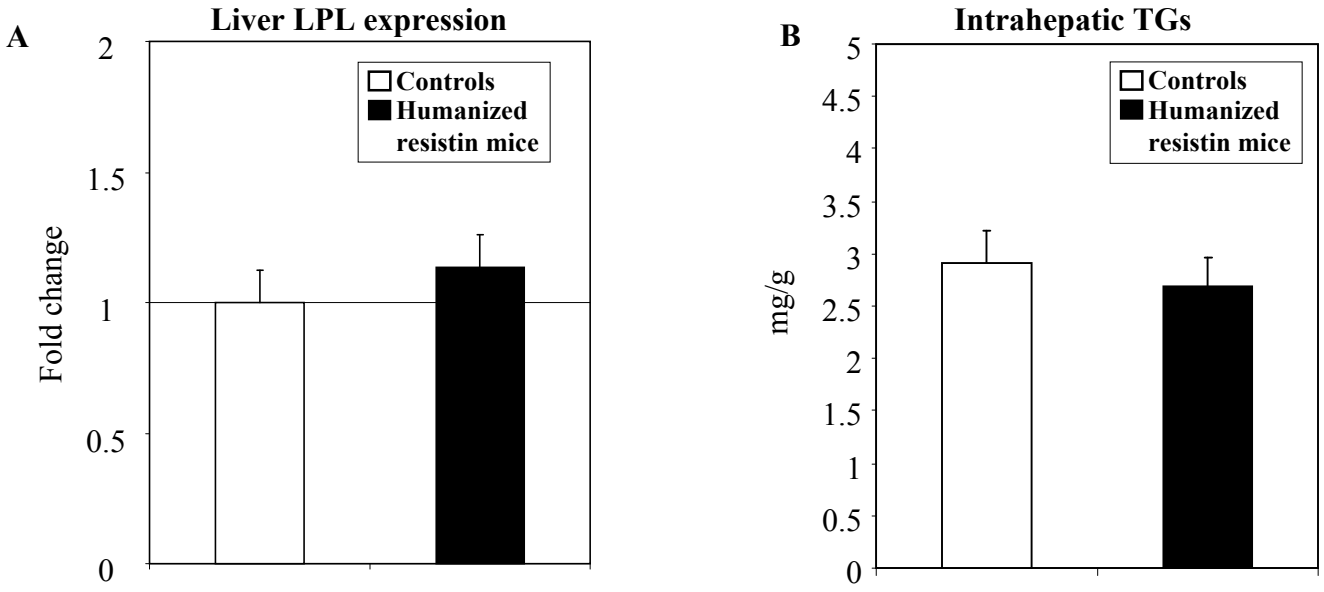

Figure S7. Humanized resistin mice show no difference in liver phenotype. (**A**) Liver LPL gene expression analysis shows no difference between humanized resistin mice and controls. (**B**) There was no difference in intrahepatic triglycerides concentration between the humanized resistin mice and controls. *LPL:* Lipoprotein Lipase, Data are expressed as mean ± SEM; $n = 9$.

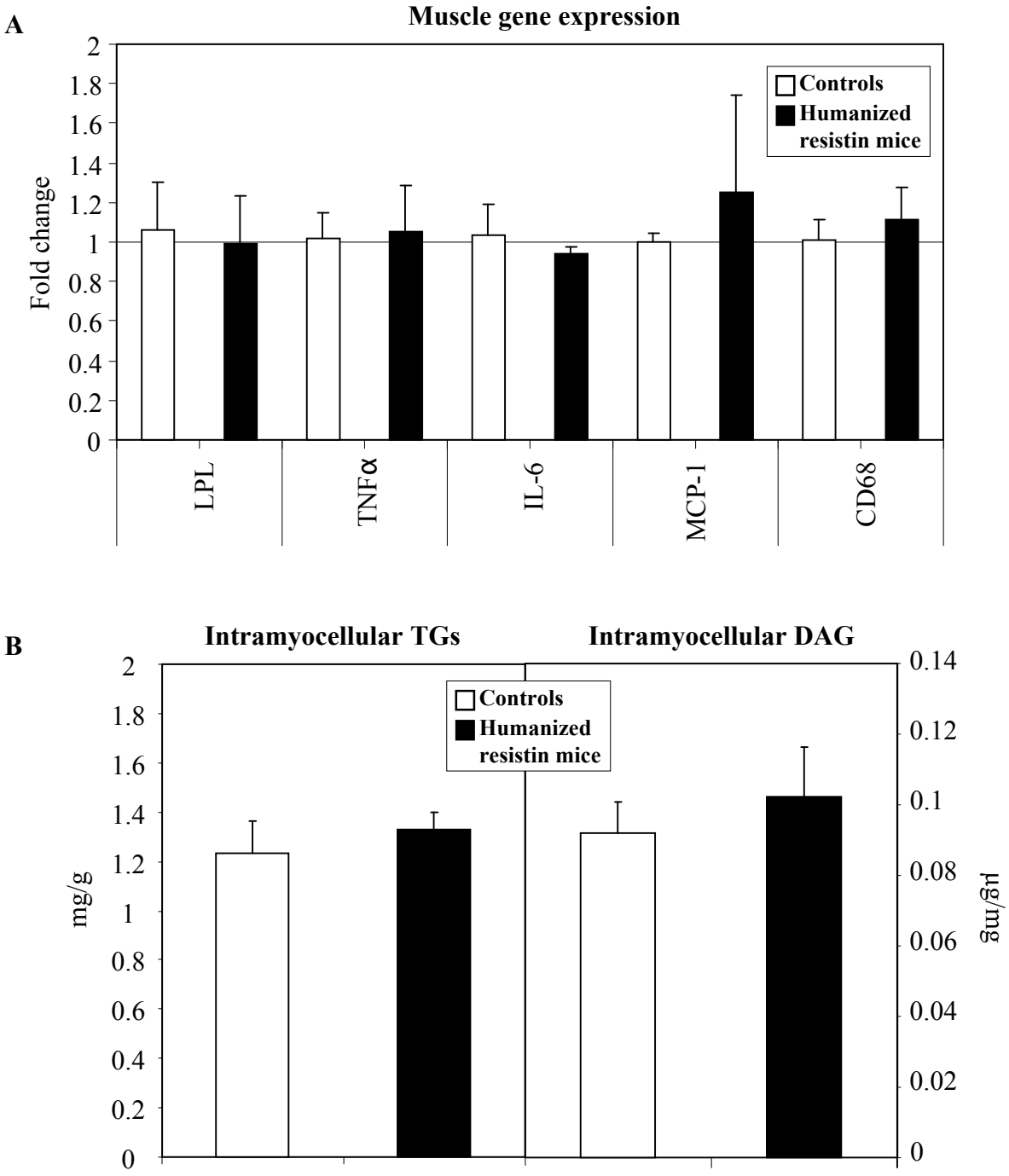

Figure S8. Humanized resistin mice show no difference in muscle gene expression or the accumulation of muscle lipid and lipid derived metabolites when put on a short term (4 days) high fat diet. (**A**) Analysis of muscle of humanized resistin and control mice on short term high fat diet shows no change in gene expression between the two groups. (**B**) Intramyocellular triglyceride concentration in skeletal muscle (left panel) and Intracellular muscle DAG levels (right panel) of humanized resistin mice on short term high fat. *LPL:* Lipoprotein Lipase, *MCP-1:* Monocyte chemotactic protein-1, *TGs*: Triglycerides, *DAG*: Diacyglycerols. Data are expressed as mean ± SEM; $n = 6$, .

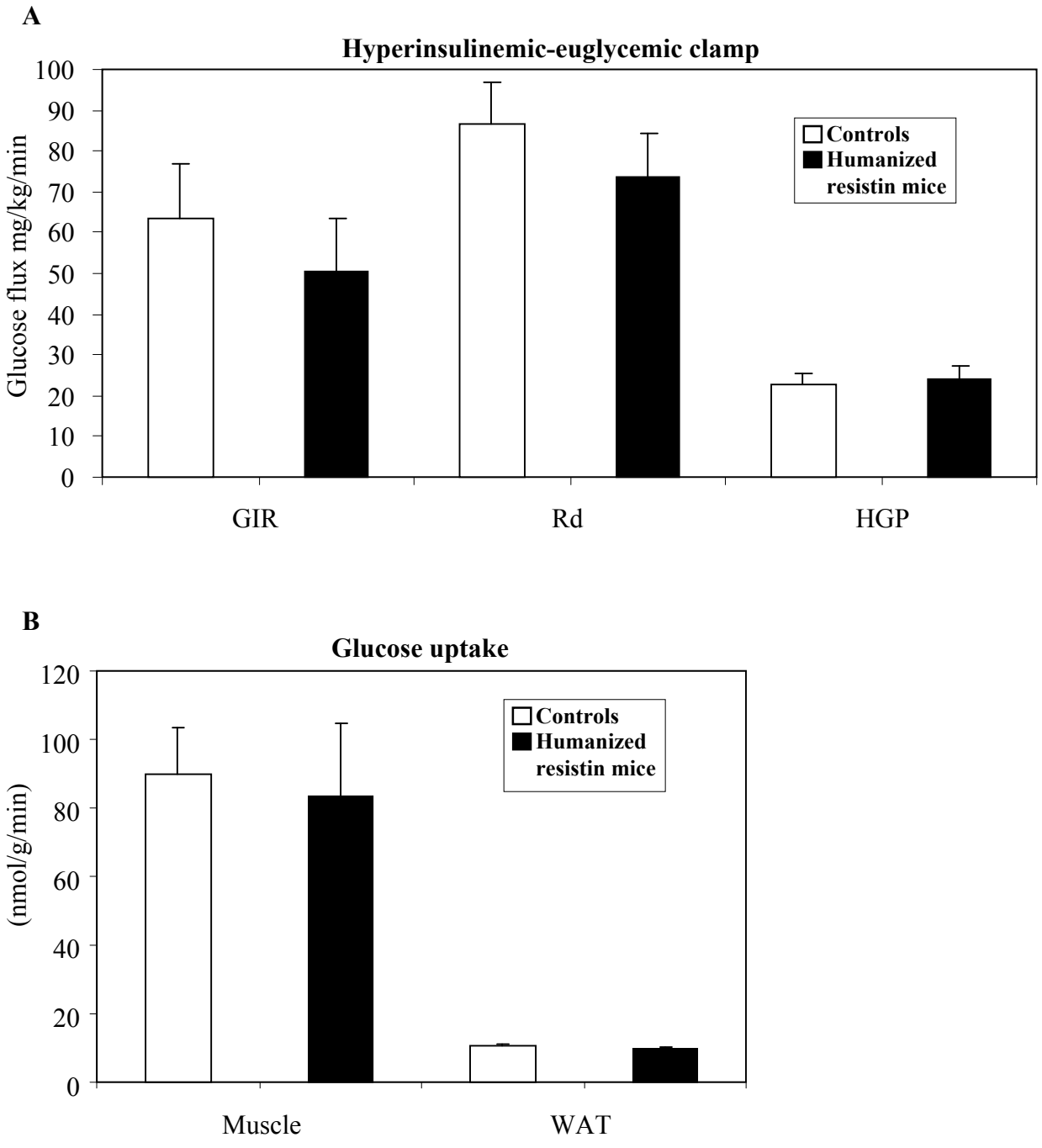

Figure S9. The humanized resistin mice show no difference in glucose homeostasis from controls when put on short term (4 days) high fat diet. (**A**) Hyperinsulinemic-euglycemic clamp analysis of humanized resistin mice v. controls on short term high fat diet. (**B**) Rate of insulin-stimulated glucose uptake in muscle and WAT in mice on high fat diet for 4 days. *GIR:* glucose infusion rate, *Rd:* rate of glucose disposal, *HGP:* hepatic glucose production, *WAT:* white adipose tissue. Data are expressed as mean ± SEM; $n = 4$.